Energy Release During Slow Long Duration Flares Observed by RHESSI

U. Bąk-Stęślicka, T. Mrozek and S. Kołomański

Astronomical Institute, University of Wrocław, ul. Kopernika 11, 51-622 Wrocław, Poland email: bak,mrozek,kolomanski@astro.uni.wroc.pl

Abstract. Slow Long Duration Events (SLDEs) are flares characterized by long duration of rising phase. In many such cases impulsive phase is weak with lack of typical short-lasting pulses. Instead of that smooth, long-lasting Hard X-ray (HXR) emission is observed. We analysed hard X-ray emission and morphology of six selected SLDEs. In our analysis we utilized data from RHESSI and GOES satellites. Physical parameters of HXR sources were obtained from imaging spectroscopy and were used for the energy balance analysis. Characteristic time of heating rate decrease, after reaching its maximum value, is very long, which explains long rising phase of these flares.

Keywords: Sun: corona - flares - X-rays

1. Introduction

A Long Duration Event (LDE) is a flare characterized by slow decrease of Soft X-ray (SXR) emission. SXR images of such flares were observed since *Skylab* and *Solar Maximum Mission* (SMM) observations (Sheeley *et al.*, 1975). Those observations indicated that LDEs usually occurred in high arcade of loops (Kahler, 1977). *Yohkoh* observed flares with better than *Skylab* and SMM temporal and spatial resolution, so that LDEs became the object of study by many authors (Tsuneta *et al.*, 1992; Feldman *et al.*, 1995; Hudson, Acton, and Freeland, 1996; Tomczak, 1997; Harra-Murnion, Schmieder, and van Driel-Gesztelyi, 1998; Isobe *et al.*, 2002; Phillips, Feldman, and Harra, 2005b; Kołomański, 2007a; Kołomański, 2007b).

Among LDEs are flares with rise phase lasting longer than in others, *i. e.* more than 30 minutes. Such flares are called Slow Long Duration Events (SLDEs) and their characteristic feature is that their impulsive phase is weak or does not exist (Hudson and McKenzie, 2000; Hudson and McKenzie, 2001). In many cases long-lasting Hard X-ray (HXR) emission was observed and its non-thermal character was confirmed (Hudson and McKenzie, 2000). During *Yohkoh* mission (1991 − 2001) *Geostationary Operational Environmental Satellites* (GOES) registered more than 250 SLDEs (Bąk-Stęślicka, 2007). The well known examples of slow LDE are 1992 February 21 (Tsuneta *et al.*, 1992) and 1999 January 20 events in which supra-arcade downflows were discovered (McKenzie and Hudson, 1999; McKenzie, 2000).

GOES observations were useful for finding SLDEs. In the paper of Bąk-Stęślicka and Jakimiec (2005) it has been shown that time interval, Δt, between the temperature and emission measure maxima, can be used as a measure of duration of rising phase. This method is independent of background level and gives us more reliable value of the duration of rising phase.

In the work Bąk-Stęślicka (2007) *Yohkoh* Hard X-ray Telescope (HXT, Kosugi *et al.*, 1991) data were used to analyse several limb or near-the-limb slow LDEs. In most of the cases long-lasting HXR emission with lack of typical, short lasting pulses was observed. HXR emission in low energy channel was spatialy correlated with tops of loops seen in SXR images. In a few cases high energy emission sources were observed near footpoints of loops.

In the paper of Bąk-Stęślicka and Jakimiec (2005) *Yohkoh* Soft X-ray Telescope (SXT, Tsuneta *et al.*, 1991) images were used to analyse morphology of loop-top sources (LTS) and to calculate their physical parameters. This analysis indicated that most of the slow LDEs occurred in high or mid-high structures ($h \sim 20 - 50$ Mm). The loop-top sources were characterized by low temperature ($T < 10$ MK), low density ($N \sim 10^{10}\,\mathrm{cm}^{-3}$) and large size ($r > 7 \times 10^8$ cm). The thermal energy release rate was small, below $1\,\mathrm{erg\,cm}^{-3}\mathrm{s}^{-1}$ and decreased very slowly with time after reaching its maximum value.

Slow LDEs could not be investigated in more detail because of limited sensitivity of SXT telescope and low spectral resolution of HXT telescope. To overcome these instrumental limitations we decided to use *Reuven Ramaty High Energy Solar Spectroscopic Imager* (RHESSI) observations. RHESSI allows us to investigate spatially resolved HXR emission of SLDEs with 1keV energy resolution, distinguish between the thermal and non-thermal nature of an LTS and calculate its physical parameters. Here we present analysis of six selected slow LDEs.

2. Observations

Our analysis is based on RHESSI (Lin *et al.*, 2002) and GOES X-ray Sensor (XRS) data supported by *Solar and Heliospheric Observatory* Extreme UV Imaging Telescope (SOHO/EIT, Delaboudini'ere *et al.*, 1995), *Transition Region and Coronal Explorer* (TRACE, Handy, Acton, and Kankelborg, 1999) and GOES Solar X-Ray Imager (SXI, Hill *et al.*, 2005) observations. RHESSI is a rotating Fourier imager with nine detectors made of pure germanium crystals (Lin *et al.*, 2002). The detectors record energy and time of arrival for each HXR photon detected. Pairs of grids placed

ahead of the detectors and the rotation of the whole satellite (4 s period) cause modulation of HXR radiation coming from solar sources. It is possible to reconstruct HXR images (Hurford, Schmahl, and Schwartz, 2002) using several available algorithms.

We analysed rise phase of SLDE events using images reconstructed with PIXON algorithm (Puetter and Yahil, 1999 and references within). The images were reconstructed in time intervals of $20 - 40$ s covering the whole rise phase. Energy intervals were narrow, usually $1 - 2$ keV. Such intervals were chosen since we were interested in the image spectroscopy of observed HXR sources. The image spectroscopy we performed has an advantage in comparison to "standard" spectroscopy based on the fluxes measured for the whole Sun. Namely, for the rotating Fourier imager the background photons do not influence modulation profile, the analysis of fluxes can be done more precisely.

3. Data Analysis

For our analysis we selected six limb or near-the-limb solar flares with slow rise phases (the rise phases lasted between 25–150 minutes). We calculated temperature T_G, emission measure EM_G and time difference, Δt, between their maxima using GOES/XRS data. We obtained physical parameters of loop-top sources using RHESSI data.

3.1. Physical Parameters of LTS

A loop-top source was defined as an area of HXR emission bounded by the intensity isoline equal to 50% of intensity of the brightest pixel. We calculated the source area for a given time interval and different energy ranges. The mean area was used for calculating the mean radius, r, assuming the spherical shape of the loop-top source. Using the mean radius (Table II) we calculated the volume of emitting region for a given time interval. The altitude of the loop-top source was calculated from centroids of the HXR emission source.

With spatially resolved signals we were able to perform spectroscopy of individual HXR sources (bounded by isocontour equal to 50% of intensity of brightest pixel) using standard OSPEX package. The best fit to the observed spectra was obtained with a use of thermal, two spectral line complexes (at 6.7 keV and 8.0 keV) and single power-law components. Other sets of components, for example double thermal despite thermal plus power-law, were also used. In such cases the obtained fits were significantly worse. The values obtained for T_R and EM_R were used to calculate heating rate during the rise phase of investigated flares.

Uncertainties in investigated parameters were calculated as follows. In the case of SLDEs we may assume slow temporal changes of the parameters. Thus, observed fast and small fluctuations of the parameters observed for consecutive time intervals may be the product of observational errors. After subtracting a slow-varying trend in: size of the loop-top sources, temperature and emission measure we calculated a standard deviation for them. We treated the standard deviation as an uncertainty of the parameters. The obtained estimations for uncertainties are: about 5% for the mean radius of the loop-top source, about 15% for the volume of LTS, less than 5% for temperature, and less than 20% for emission measure.

A non-thermal component of the HXR spectrum was observed in four cases. We fitted this component with a double power-law function. We treated a break energy and power law index above this energy as free parameters. The power law index below the break energy was fixed at constant value. The total power in non-thermal electrons above cut-off energy, ϵ_c, was calculated using a formula given by Aschwanden, 2005:

$$P\left(\epsilon \geq \epsilon_c\right) = 4.3 \times 10^{24} \frac{b\left(\gamma\right)}{\left(\gamma - 1\right)} A\left(\epsilon_c\right)^{-(\gamma-1)} \qquad \left(\text{erg s}^{-1}\right) \qquad (1)$$

Where $b\left(\gamma\right) \approx 0.27\gamma^3$ is the auxiliary function calculated in Hudson, Canfield, and McKenzie (1978), A is a normalization factor. Since we were interested in a rough estimation of non-thermal power we assumed that break energy from our fits is close to the cut-off energy.

3.2. Energy balance

We estimated the value of the heating function, E_H, for the loop-top sources seen in RHESSI images for the all analysed flares. In order to calculate heating rate of an LTS we considered its energy balance during the rise phase. Here we consider time interval, Δt, after temperature maximum, when the energy release has begun to decrease, but the emission measure is still increasing. Three major cooling processes where included into this balance: expansion, radiation and conduction:

$$\left(\frac{d\mathcal{E}}{dt}\right)_{obs} = \left(\frac{d\mathcal{E}}{dt}\right)_{ad} - E_C - E_R + E_H \qquad (2)$$

where: $\mathcal{E} = 3NkT$ is thermal energy density, $\left(\frac{d\mathcal{E}}{dt}\right)_{obs}$ is the decrease of $\mathcal{E}$ per second estimated from temperature (T) and density (N) values, $\left(\frac{d\mathcal{E}}{dt}\right)_{ad}$ is the decrease due to the adiabatic expansion of plasma in a source, E_C is the energy loss due to thermal conduction, E_R is the radiative loss, and E_H is the heating rate or thermal energy release. The values of E_C, E_R and E_H are in erg cm^{-3} s^{-1}. We calculated:

- $\left(\frac{d\mathcal{E}}{dt}\right)_{ad} = 5kT\left(\frac{dN}{dt}\right)$,

- $E_C = 3.9 \times 10^{-7} T^{3.5}/(Lr)$, where r is the LTS radius and L is loop semi-length (Jakimiec et $al.$, 1997).

- $E_R = N^2\Phi(T)$, where $\Phi(T)$ is the radiative loss function taken from Dere et $al.$ (2009).

We took the height of an LTS above the photosphere, h, as an approximation for L in the expression for E_C. Since the value of h is always smaller than L thus, the calculated value of E_H is the upper limit.

Uncertainties calculated for basic parameters allowed us to estimate the errors in the E_H. In the case of SLDEs E_C is a dominant contributor in energy balance. It is about an order of magnitude greater than other contributors to the E_H. The estimated value of the uncertainty of E_C is about 20%. Similar value have been obtained through the analysis of a standard deviation.

For all selected flares we analysed time evolution of $E_H(t)$ and calculated characteristic time τ of the $E_H(t)$ decrease after reaching its maximum value:

$$\frac{1}{\tau} = \frac{dlnE_H(t)}{dt} \tag{3}$$

Table I. Data for selected flares

| Flare | Date | GOES/XRS | | | | | |
		Start [UT]	Max [UT]	class	T_{Gmax} [MK]	EM_{Gmax} [10^{48}cm^{-3}]	Δt [min]
1.	2003 Oct. 24	02:19	02:54	M7.6	17.8	43	21
2.	2003 Nov. 18	09:23	10:11	M5.4	12.8	29	23
3.	2005 Jul. 13	14:01	14:49	M5.0	19.0	26	39
4.	2005 Aug. 23	14:19	14:44	M2.7	20.2	14	20
5.	2005 Sep. 06	19:32	22:02	M1.4	16.2	7.7	101
6.	2007 Jan. 25	06:33	07:14	C6.3	13.0	5	29

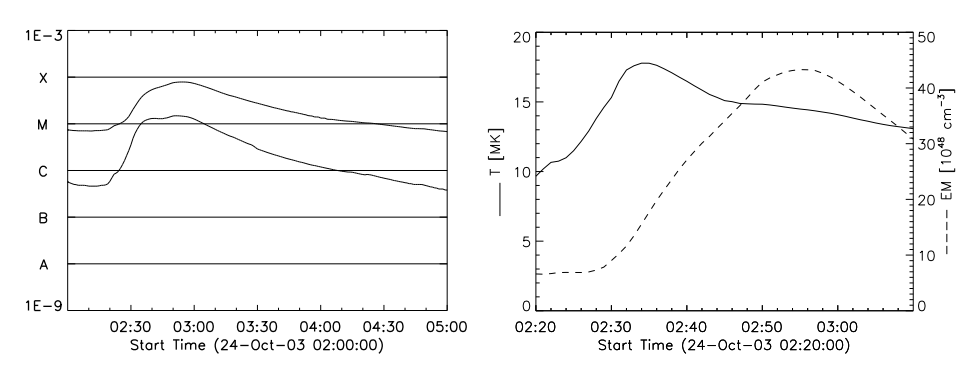$\Delta t = t(EM_{Gmax}) - t(T_{Gmax})$

Figure 1. Left: GOES X-ray fluxes (upper curve: $1 - 8$ Å, lower curve: $0.5 - 4$ Å). *Right:* Temperature and emission measure during the rise phase of the 2003 October 24 flare obtained from the GOES/XRS data.

4. Results

We calculated temperature, T_G, emission measure, EM_G, and difference between their maxima (Table I) using GOES/XRS data. For all flares we used RHESSI data to obtain physical parameters of loop-top sources from spectra fitting. The parameters were used to determine heating rate and characteristic time of its decrease after reaching maximum value. Below we describe three flares in details. Results for all flares are given in Table II.

4.1. 2003 OCTOBER 24 FLARE

The flare started at about 02:19 UT in active region NOAA 10486. SXR flux reached its maximum (M7.6) at 02:54 UT. Two phases are clearly seen (see Figure 1, left panel) in the GOES light curves. First one from the beginning up to ∼02:44 UT, the second one after 02:44 UT. We used GOES/XRS data to calculate temperature, T_G, and emission measure, EM_G, of the whole flare. Temperature increased slowly and reached its maximum value (17.8 MK) at 02:34 UT (Figure 1, right panel). Emission measure reached its maximum value (43×10^{48} cm^{-3}) at 02:55 UT. Difference, Δt, between these two maxima equals 21 minutes.

   The flare was well observed by many instruments. Detailed multi-wavelength analysis of this flare was presented by other authors (Li and Li, 2008; Joshi *et al.*, 2009). Two phases of this flare are also visible in the RHESSI light curves (Figure 2, left panel).

4.1.1. *First phase*
RHESSI observed this flare from 02:22 UT. During the first phase emission up to $25 - 50$ keV range was observed, there were no short-lasting pulses.
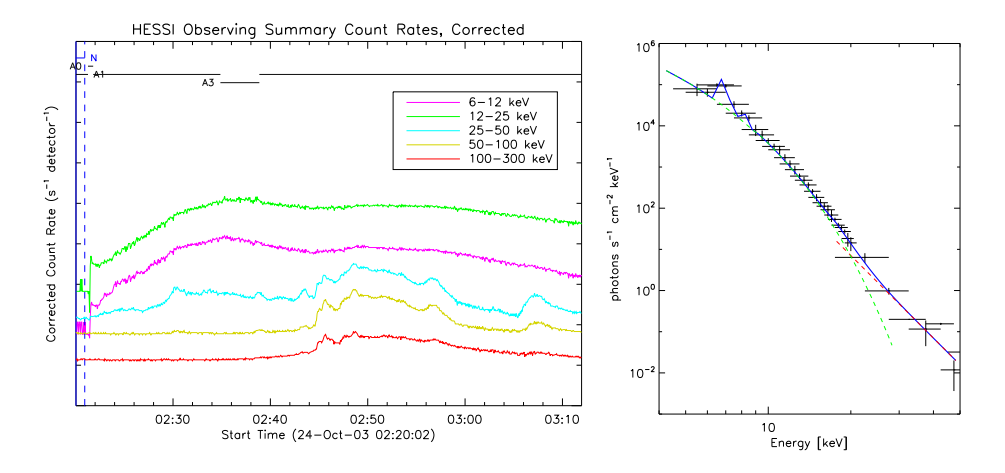
Figure 2. *Left:* RHESSI light curves of the 2003 October 24 flare. *Right:* The RHESSI X-ray spectrum of the loop-top source (source N) observed during the 2003 October 24 flare at 02:48 UT (horizontal bars corresponds to the energy bin widths). This spectrum was fitted using the thermal component (green curve), two spectral line complexes (at 6.7 keV and 8.0 keV) and single power-law component (red curve). The sum of all these models, the best-fit model, is represented by the blue curve.
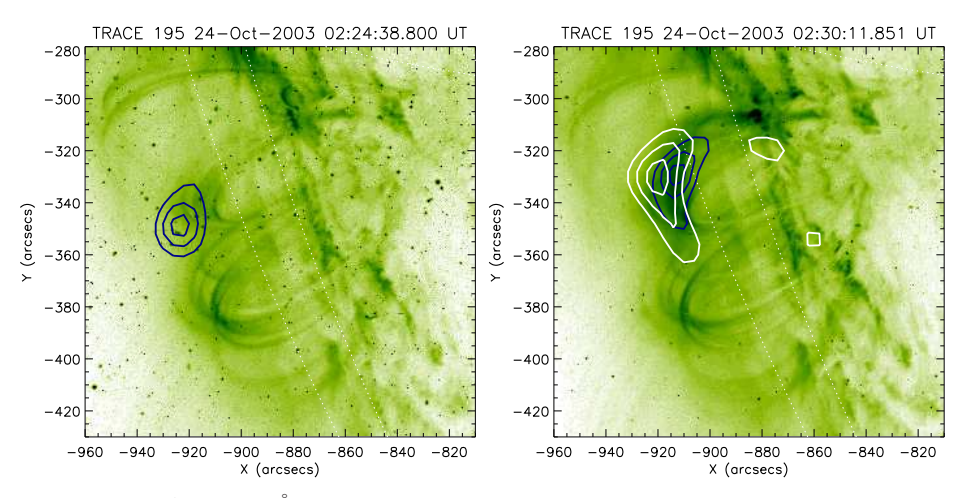

Figure 3. TRACE 195 Å images showing 2003 October 24 flare during the first phase. Contours show the emission in the $10 - 11$ keV range (*blue*) and $20 - 25$ keV range (*white*) observed with RHESSI. The contours are for 50%, 70% and 90% of maximum emission.

TRACE data helped us to investigate morphology of the flare. Thermal response function for TRACE 195 Å filter has two distinct maxima: higher for plasma at $T \sim 1 - 2$ MK and lower for significantly hotter plasma ($T \sim 10 - 30$ MK, Phillips, Chifor, and Landi, 2005a). We carefully co-alignmented RHESSI and TRACE 195 Å images using SOHO/EIT 195 Å
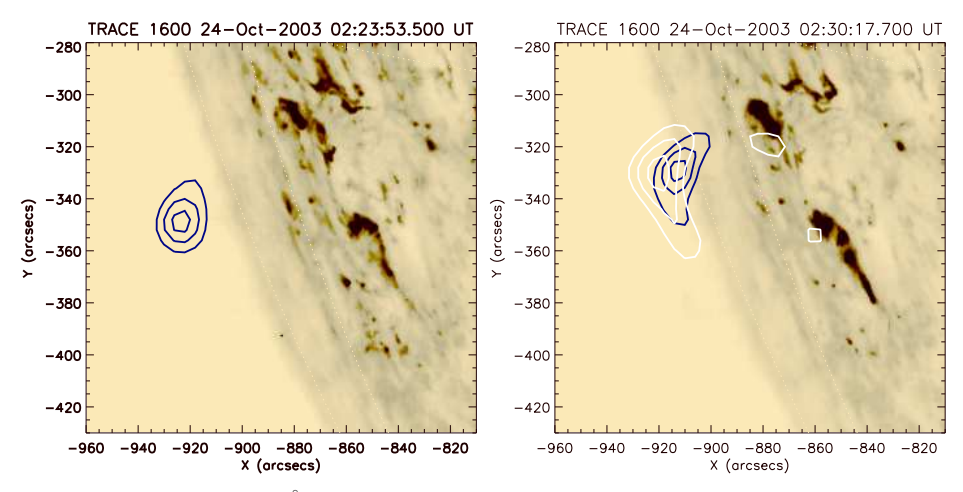
Figure 4. TRACE 1600 Å images showing 2003 October 24 flare during the first phase. Contours show the emission in the $10-11$ keV range (*blue*) and $20-25$ keV range(*white*) observed with RHESSI. The contours are for 50%, 70% and 90% of maximum emission.

images (Gallagher *et al.*, 2002). TRACE 195 Å images with RHESSI contours are shown in Figure 3. At the beginning, one source, slightly elongated in the north direction, was observed. A few minutes later, the source (source N) was visible at lower altitude (see Table II) and was spatially correlated with the very bright loop-top source seen in the TRACE 195 Å images. The hot source N dominated in the emission during the first phase. Shrinkage of TRACE and RHESSI loops was previously reported (Li and Li, 2008; Joshi *et al.*, 2009). Only at about 02:30 UT footpoints (FPN – in north direction, FPS – in south direction) were visible and were spatially correlated with the ribbons seen in TRACE 1600 Å images (Figure 4).

4.1.2. *Second phase*
The second phase started at about 02:44 UT and lasted after flare maximum. Emission in energy range of $100-300$ keV range was observed during this phase. Emission in lower energy range was dominated by source N, which was observed up to $30-35$ keV. At flare maximum second source, S, was observed and brightened with time (Figure 5). Several minutes after the maximum of the flare, the source S dominated emission in energy up to 25 keV. For some time we observed only one elongated source and there was no possibility to separate it into sources N and S. The emission from footpoints was very strong, especially at the beginning of the second phase (Figure 6). Separation between footpoints was smaller than during the first phase. At the beginning of the second phase FPN was stronger than FPS and was observed in energy range up to $200-300$ keV. FPS was observed in the
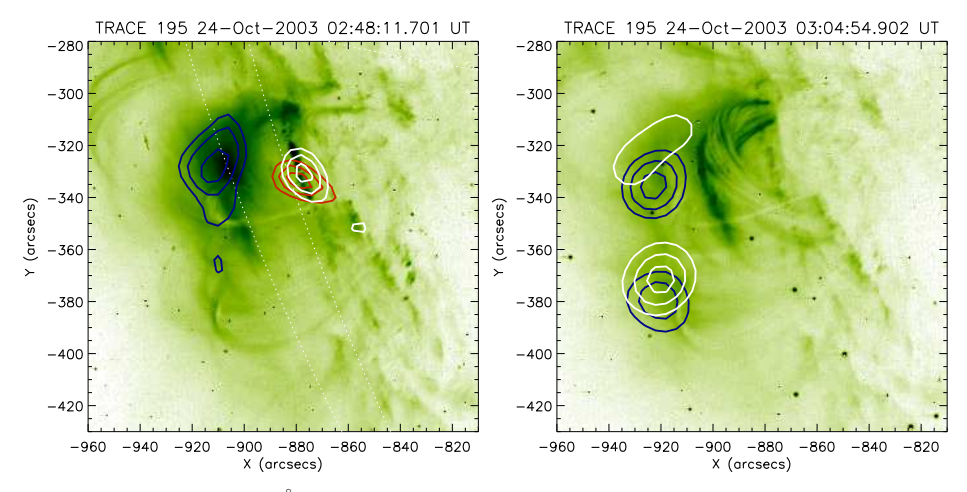
Figure 5. TRACE 195 Å images showing the 2003 October 24 flare during the second phase. Contours show the emission in the $10-11$ keV range (*blue*), $20-25$ keV range(*white*) and $100-120$ keV range (*red*) observed with RHESSI. The contours are for 50%, 70% and 90% of maximum emission.
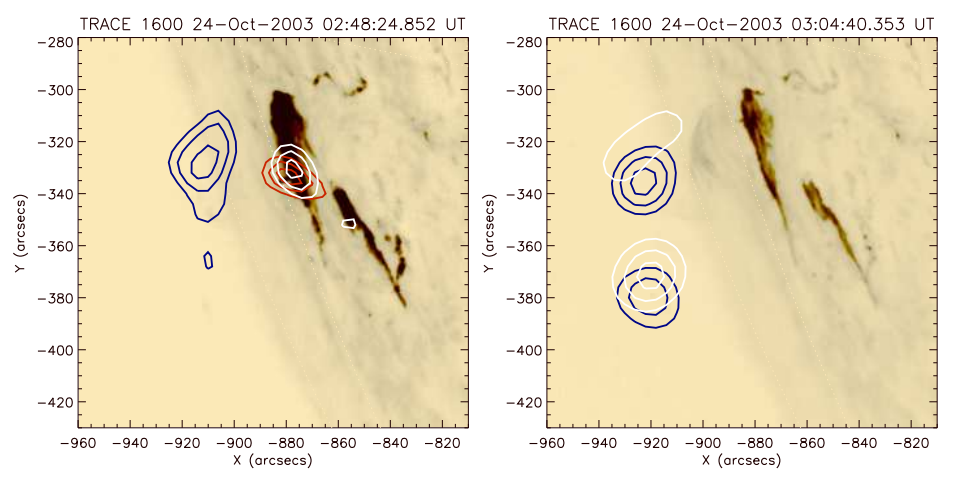

Figure 6. TRACE 1600 Å images showing the 2003 October 24 flare during the second phase. Contours show the emission in the $10-11$ keV range (*blue*) and $20-25$ keV range(*white*) and $100-120$ keV range (*red*) observed with RHESSI. The contours are for 50%, 70% and 90% of maximum emission.

energy range up to $70-80$ keV after flare maximum (at about 03:07–03:08 UT).

4.1.3. *Physical parameters*

We calculated temperature, T_R, emission measure, EM_R, and non-thermal energy parameters of both LTSs from imaging spectroscopy (see example spectrum in Figure 2, right panel). The source N was observed during the

whole rising phase and was brighter than source S during most of the time. Plasma in the LTS N was hot at the beginning, $T_R > 25$ MK, and less hot after the flare maximum, $T_R \sim 16$ MK, (Table II). Heating rate was also very high ($E_H > 15$ erg cm^{-3}s^{-1} at the beginning and $E_H < 2.5$ erg cm^{-3}s^{-1} after the flare maximum). This value of heating rate is much higher than values obtained from *Yohkoh* observations, due to weak *Yohkoh*/SXT sensitivity to higher temperature plasma. After reaching its maximum value (at the beginning of the flare), heating rate decreased with characteristic time $\tau = 1240$ s. Rate of the non-thermal energy release per unit volume for source N was about 5 erg cm^{-3}s^{-1} during the rising phase.

The source S was observed mostly during the second phase. Maximum value of temperature of LTS S was ~ 21 MK and decreased very slowly to ~ 18 MK after flare maximum. After flare maximum the source S remains hotter and brighter than the source N and became dominant source.

4.2. 2003 November 18 flare

The flare occurred in active region NOAA 10506 at the eastern solar limb. It began at 09:23 UT. SXR flux increased slowly and reached its maximum value (GOES class M4.5) at 10:11 UT (Figure 7, left panel). GOES fluxes were used to calculate temperature, T_G, and emission measure, EM_G, and time shift between their maxima. Temperature increased slowly and reached its maximum value (12.8 MK) at 09:51 UT (Figure 7, right panel). After that, temperature slightly dropped (down to 11 MK). After 10:30 UT, T_G slighty increased which was related to additional emission, seen on GOES light curve after the maximum. Emission measure reached its maximum value (29×10^{48} cm^{-3}) at 10:14 UT. Time difference between T_G and EM_G maxima is equal to 23 minutes.
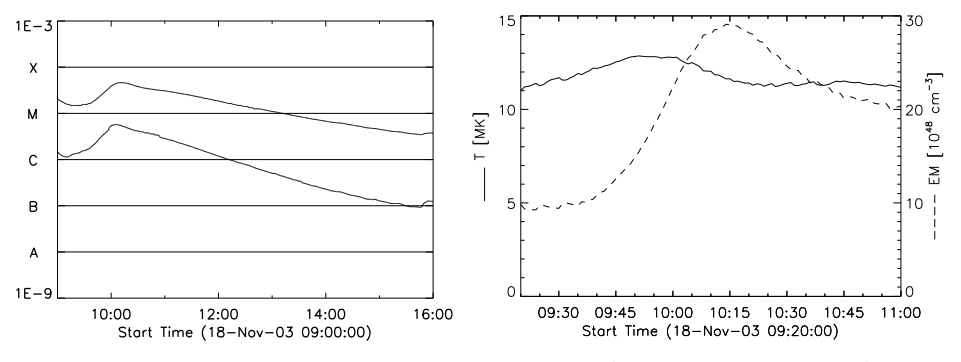

Figure 7. Left: GOES X-ray fluxes (upper curve: $1 - 8$ Å, lower curve: $0.5 - 4$ Å). *Right:* Temperature and emission measure during the rise phase of the 2003 November 18 flare obtained from the GOES/XRS data.
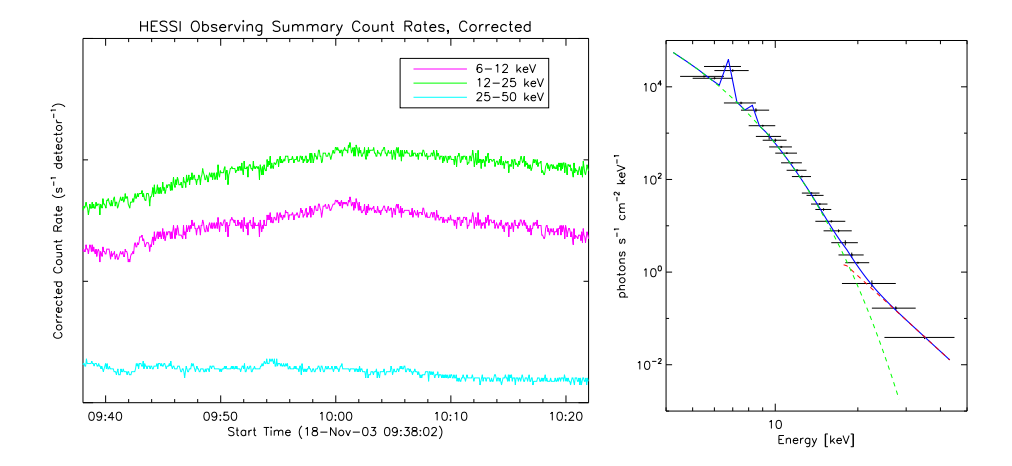
*Figure 8. Left:*RHESSI light curves for the 2003 November 18 flare.*Right:* The RHESSI X-ray spectrum of the loop-top source observed during the 2003 November 18 flare at 09:46 UT (horizontal bars corresponds to the energy bin widths). This spectrum was fitted using the thermal component (green curve), two spectral line complexes (at 6.7 keV and 8.0 keV) and single power-law component (red curve). The sum of all these models, the best-fit model, is represented by the blue curve.
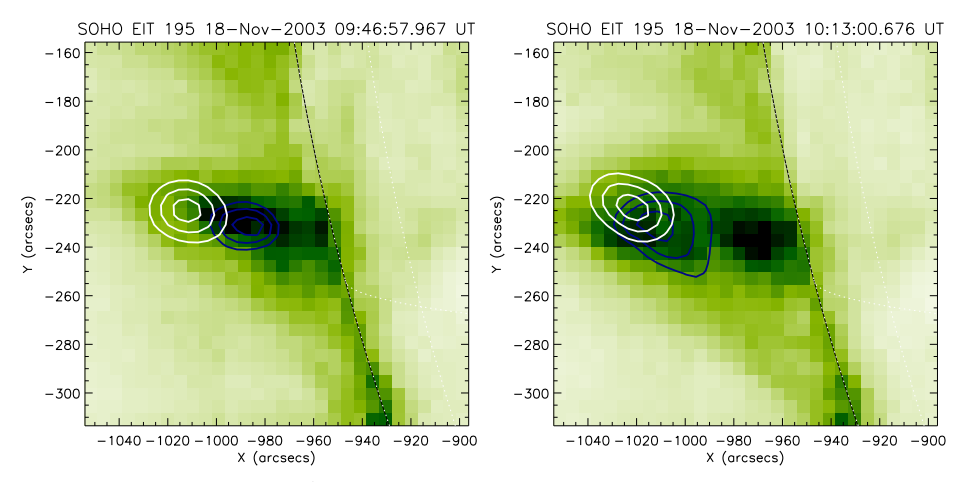

Figure 9. SOHO/EIT 195 Å images showing flare of the 2003 November 18 during the rise phase. Contours show the emission in the $10-11$ keV range (*blue*) and $20-25$ keV (*white*) observed with RHESSI. The contours are for 50%, 70% and 90% of maximum emission.

RHESSI observed the flare during almost entire rise phase (see Figure 8). Short-lasting pulses were not observed. Only long-lasting emission in energy range up to 25 keV was observed most of the time. However, for a few moments of time very weak emission in energy range $25-50$ keV was also observed.

In the PIXON images only a loop-top source was observed. This source was spatially correlated with the limb structure seen in the SOHO/EIT images (Figure 9). Only footpoints of the loops were occulted. The whole structure became visible in the EIT images a few hours after flare maximum, due to the Sun rotation. The structure expanded and a few hours after flare maximum high arcade of loops was observed. We obtained the location of the HXR source, its size and height above the photosphere from PIXON images. Emission at higher energy range (> 20 keV) was observed at higher altitude (Figure 9). Therefore we calculated average value of height at each moment of time. The average height increased during the rise phase from $h \sim 20$ Mm to $h \sim 50$ Mm. We calculated temperature, T_R, emission measure, EM_R, and non-thermal component parameters from the spectra fitting (see Figure 8, right panel). Temperature decreased slowly (~ 19 MK at the beginning, ~ 17 MK at maximum), which is characteristic feature of SLDE flares. Physical parameters obtained (see Table II) allowed us to calculate thermal energy release rate ($E_H \sim 5$ erg cm^{-3}s^{-1} at the beginning, ~ 1 erg cm^{-3}s^{-1} at the maximum).

During the rise phase loop-top source was visible up to 40 keV and its emission showed clear non-thermal component. At about 09:54–09:55 UT rate of the non-thermal energy release per unit volume was about 0.3 erg cm $^{-3}$ s^{-1}.

4.3. 2005 September 6 flare

The flare of 2005 September 6 occurred in an active region NOAA 10808, $\sim 6°$ behind the eastern solar limb. The flare (GOES class M1.4) started at 19:32 UT and reached its maximum at 22:02 UT (Figure 10, left panel). Temperature obtained from the GOES/XRS data increased for almost 50 minutes and reached maximum (16.2 MK) at 20:23 UT. Decrease of temper-
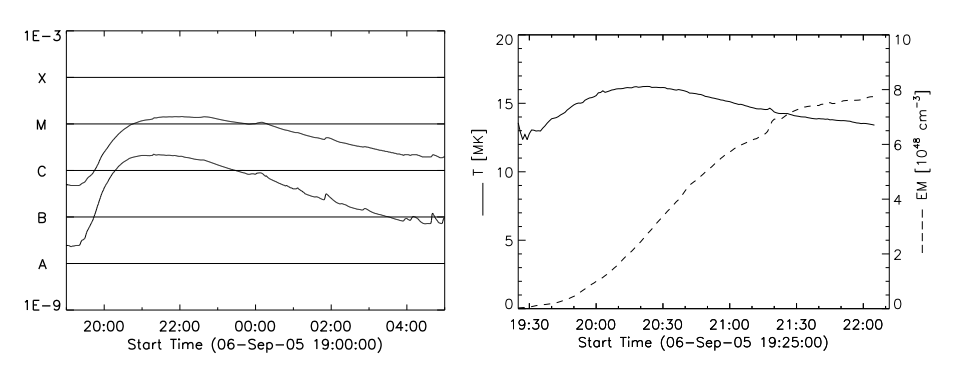

Figure 10. Left: GOES X-ray fluxes (upper curve: $1 - 8$ Å, lower curve: $0.5 - 4$ Å). *Right:* Temperature and emission measure during the rise phase of the 2005 September 6 flare obtained from the GOES data.
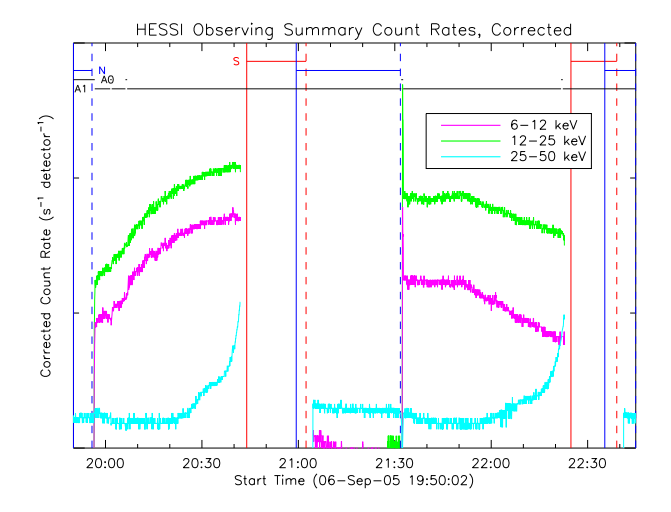
Figure 11. RHESSI light curves for the September 6, 2005 flare.

ature during the rise phase of the flare was very slow (see Figure 10, right panel). Maximum value of emission measure (7.7×10^{48} cm^{-3}) was at 22:02 UT. Time difference between these two maxima is equal to 101 minutes, which is the largest Δt we have found.

During the rise phase long-lasting HXR emission up to 25 keV was observed (Figure 11) without short-lasting pulses. This flare was slightly occulted, only footpoints were behind the limb. The HXR emission source is visible above a loop seen in the SXI image (Figure 12, left panel). TRACE observations (3 hours after flare maximum) show arcade of loops located near the limb, with loops oriented along the line of sight, which explains "cusp-like" shape seen in SXI images. From the RHESSI PIXON images we determined size of the LTS ($\sim 16 - 20$ Mm) and its height above the photosphere (> 70 Mm). The results are shown in Table II. We performed imaging spectroscopy to obtain physical parameters of the LTS. A spectrum with fitted model (thermal component plus lines at 6 keV and 8 keV) is shown in Figure 12, right panel. Temperatures obtained (~ 20 MK at the beginning and ~ 15 MK at the maximum) are higher than those obtained from the GOES/XRS data which is due to a different temperature sensitivity of these two instruments. Slow changes of temperature are common feature for GOES and RHESSI observations of this flare. Obtained temperature and emission measure (from spectra fitting), size of LTS and height above the photosphere (from images) allowed us to calculate energy balance. Value of heating rate obtained is low (Table II) and decreases with the characteristic time of 4430 s, which explains very long rising phase.
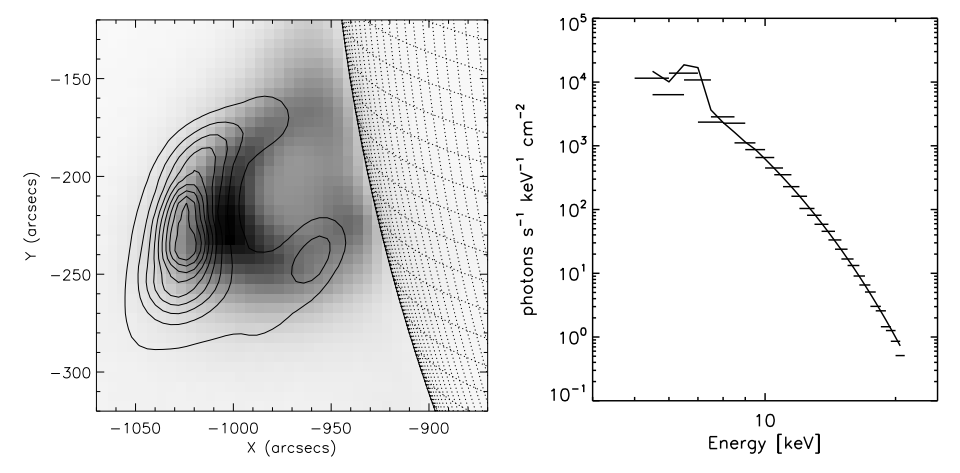
Figure 12. Left: GOES/SXI image showing 2005 September 6 flare during the rise phase. Contours show the emission in the $8 - 9$ keV range observed with RHESSI. The contours are for 10%, 20%, 30%, 40%, 50%, 60%, 70%, 80% and 90% of maximum emission. *Right:* The RHESSI X-ray spectrum of the loop-top source observed during the 2005 September 6 flare at 20:37 UT (horizontal bars corresponds to the energy bin widths). This spectrum was fitted using the thermal component and two spectral line complexes (at 6.7 keV and 8.0 keV). The sum of all these models, the best-fit model, is represented by the black curve.

5. Summary

Slow Long Duration Events are flares characterized by long rising phase and smooth HXR emission. We used RHESSI and GOES/XRS data to obtain physical parameters of loop-top sources of such flares. TRACE, SOHO/EIT and GOES/SXI images helped us to investigate morphology of the flares.

Our analysis can be summarized as follows:

— Using RHESSI and GOES/XRS observations, we have confirmed that characteristic feature of the SLDEs is a large time interval, $\Delta t > 20$ minutes, between maximum of temperature and maximum of emission measure.

— As other LDEs, slow LDEs often occur in arcade of loops. Height of these structures are high ($h \sim 25 - 50$ Mm).

— In almost all cases (except flare No. 4) long-lasting HXR emission was observed. Flare with the longest rise phase (No. 5) was $\sim 6°$ behind the limb so we did not observe footpoints. In four cases (No. 1, 2, 3, 4), non-thermal emission from the loop-top sources was also observed.

— In flares No. 3 and 4 rate of non-thermal electron energy release per unit volume (from LTS) was comparable to the heating rate.

– For all analysed flares we calculated value of thermal energy release rate. Obtained values of E_H are larger than those previous obtained from SXT data (Bąk-Stęślicka and Jakimiec, 2005). This difference is caused by the fact that SXT telescope had limited sensitivity to higher temperature plasma (> 10 MK) which usually led to underestimation of flare temperature. RHESSI data enable us to estimate much more reliable (higher) values of plasma temperature and therefore higher values of E_H.

– We calculated characteristic time τ of heating function decrease after reaching its maximum value. Long duration of the SLDEs rising phase is consistent with a very slow decrease of the E_H during that phase. In most cases characteristic time of E_H decrease is larger than 1000 s. We obtained the highest value of τ for the flare with the longest rising phase (No. 5). We obtained the lowest value of τ for the flare with the shortest rise phase (No. 4).

– Assuming E_H equal to minimum value of E_H calculated for the rising phase, average volume of LTS and duration od rising phase obtained from GOES/XRS data, we estimated total thermal energy released during the rising phase. In our flares total thermal energy is at least 10^{31} ergs. The same magnitude of energy is released during the decay phase of LDEs (Kołomański, Mrozek, and Bąk-Stęślicka, 2011). This value is larger than value of total thermal energy released during rise phase of short-rising flares (Jiang *et al.*, 2006). Those authors obtained value not higher than 10^{30} ergs.

Acknowledgements

References

Aschwanden, M. J.: 2005, *Physics of the Solar Corona*: An Introduction, Praxis Publishing (Chichester, UK) and Springer (Berlin).
Bąk-Stęślicka, U., Jakimiec, J.: 2005, *Solar Phys.* **231**, 95.
Bąk-Stęślicka, U.: 2007, *PhD Thesis*, University of Wrocław

Delaboudini'ere, J.-P., Artzner, G. E., Brunaud, J., Gabriel, A. H., Hochedez, J. F. et al.: 1995, *Solar Phys.* **162**, 19.

Dere, K. P., Landi, E., Young P. R., Del Zanna, G., Landini, M. et al.: 2009, *A&A* **498**, 915.

Donnelly, R. F., Grubb, R. N., Cowley, F. C.: 1977, NOAA Tech. Memo. ERL SEL-48.

Feldman, U., Seely, J. F., Doschek, G. A., Brown, C. M., Phillips, K. J. H. et al.: 1995, *Astrophys. J.* **446**, 860.

Gallagher, P. T., Dennis, B. R., Krucker, S., Schwartz, R. A., Tolbert, A. K.: 2002, *Solar Phys.* **210**, 341.

Handy, B.N., Acton, L.W., Kankelborg, C.C.: 1999, *Solar Phys.* **187**, 229.

Harra-Murnion, L. K., Schmieder, B., van Driel-Gesztelyi, L.: 1998, *A&A* **337**, 911.

Hill, S. M., Pizzo, V. J., Balch, C. C., Biesecker, D. A., Bornmann, P. et al.: 2005, *Solar Phys.* **226**, 255.

Hudson, H. S., Acton, L. W., Freeland, S. L.: 1996, *Astrophys. J.* **470**, 629.

Hudson, H.S., Canfield, R.C., and Kane, S.R.: 1978, *Solar Phys.* **60**, 137.

Hudson, H. S., McKenzie, D. E.: 2000, High Energy Solar Physics Workshop - Anticipating HESSI, ASP Conference Series, Vol. 206. Edited by R. Ramaty and N. Mandzhavidze, 221.

Hudson, H. S., McKenzie, D. E.: 2001, *Earth Planets Space* **53**, 581.

Hurford, G. J., Schmahl, E. J., Schwartz, R. H.: 2002, *Solar Phys.* **210**, 61.

Isobe, H., Yokoyama, T., Shimojo, M., Morimoto, T., Kozu, H. et al.: 2002, *Astrophys. J.* **566**, 528.

Jakimiec, J., Sylwester, B., Sylwester, J., Serio, S., Peres, G. et al.: 1992, *A&A* **253**, 269.

Jakimiec, J., Tomczak, M., Fludra, A., Falewicz, R.: 1997, *Adv. in Space Res.* **20**, 2341.

Jiang, Y. W., Liu, S., Liu, W., Petrosian, V.: 2006, *Astrophys. J.* **638**, 1140.

Joshi, B., Veronig, A., Cho, K.-S., Bong, S. C., Somov, B. V et al.: 2009, *Astrophys. J.* **706**, 1438.

Kahler, S.: 1977, *Astrophys. J.* **214**, 891.

Kołomański, S.: 2007a, *A&A* **465**, 1021.

Kołomański, S.: 2007b, *A&A* **465**, 1035.

Kołomański, S., Mrozek, T., Bąk-Stęślicka, U.: 2011, submitted to *A&A*.

Kosugi, T., Masuda, S., Makishima, K., Inda, M., Murakami, T. et al.: 1991, *Solar Phys.* **136**, 17.

Li, H., Li, Y.: 2008, *Adv. in Space Res.* **41**, 962.

Lin, R.P., Dennis, B.R., Hurford, G.J., Smith, D.M., Zehnder, A., et al.: 2002, *Solar Phys.* **210**, 3.

McKenzie, D. E., Hudson, H., S.: 1999, *Astrophys. J.* **519**, L93.

McKenzie, D. E.: 2000, *Solar Phys.* **195**, 38.

Phillips, K. J. H., Chifor, C., Landi, E.: 2005, *Astrophys. J.* **626**, 1110.

Phillips, K. J. H., Feldman, U., Harra, L. K.: 2005, *Astrophys. J.* **634**, 641.

Piña, R.K., Puetter, R.C.: 1993, *PASP* **105**, 630.

Puetter, R.C., Yahil, A.: 1999, Astronomical Data Analysis Software and Systems VIII, ASP Conference Series 172, 307.

Reeves, K.K., Warren, H.P.: 2002, *Astrophys. J.* **578**, 590.

Sheeley, N. R., Jr., Bohlin, J. D., Brueckner, G. E., Purcell, J. D., Scherrer, V. E. et al.: 1975, *Solar Phys.* **45**, 377.

Tomczak, M.: 1997, *A&A* **317**, 223.

Tsuneta, S., Acton, L., Bruner, M., Lemen, J., Brown, W. et al.: 1991, *Solar Phys.* **136**, 37.

Tsuneta, S., Hara, H., Shimizu, T., Acton, L. W., Strong, K. T. et al.: 1992, *PASJ* **44**, 63.

Table II. Physical parameters of LTS obtained from the RHESSI data

	Date GOES Start GOES Max	time	h (Mm)	r (Mm)	T_R (MK)	EM_R*	E_H**	τ (s)
					Loop-top source N			
		02:27	34	11.1	25.2	0.4	9.6	
		02:32	27	8.8	25.6	2.4	15.3	1240
		02:48	25	8.9	19.4	6.9	6.3	
1.	2003 Oct. 24	03:04	42	8.2	16.5	5.4	2.2	
	02:19				Loop-top source S			
	02:54	02:54	47	4.0	20.8	1.6	9.3	
		03:02	46	7.6	21.0	1.3	5.1	
		03:10	50	6.3	18.6	1.9	3.6	
2.	2003 Nov. 18	09:40	21	12.0	19.2	0.6	5.1	
	09:23	09:50	30	11.4	17.7	2.4	2.8	2110
	10:11	10:01	33	13.9	17.6	3.9	2.1	
		10:10	40	12.2	17.4	3.9	2.0	
3.	2005 Jul. 13	14:16	38	8.5	23.5	2.3	7.4	
	14:01	14:23	41	9.0	22.1	4.7	5.3	2000
	14:49	14:32	39	9.3	22.0	7.1	5.3	
		14:39	40	9.8	20.1	10.0	3.6	
4.	2005 Aug. 23	14:20	27	9.2	19.7	0.04	5.9	
	14:19	14:25	25	7.8	24.3	0.5	14.5	650
	14:44	14:29	25	7.6	21.4	2.7	11.0	
		14:33	28	7.4	20.6	3.8	7.8	
		19:58	72	19.8	20.3	0.2	1.0	
5.	6-Sep-05	20:17	72	16.4	20.8	0.4	1.3	
	19:32	20:37	77	17.7	20.4	0.8	1.1	4430
	22:02	21:34	84	19.0	16.8	1.5	0.5	
		21:49	84	19.4	16.2	1.5	0.4	
		22:05	82	20.3	15.2	1.9	0.3	
6.	2007 Jan. 25	06:47	27	12.8	15.8	0.1	1.6	
	06:33	06:55	29	12.4	13.7	1.5	1.0	1100
	07:14	07:00	29	14.0	12.9	2.4	0.7	

* EM in 10^{48}cm^{-3}

** E_H in erg cm^{-3}s^{-1}